8

Using a Second Linear Damper

… in which a second damper is introduced in the test systems and it is shown that a damper using local bus frequency can be tuned using the concept of impedance matching.

The incentive for using a second damper is that two dampers will yield more damping than one. It is expected that they can provide damping of a greater number of modes together, particularly if the dampers are far apart and are aimed at modes associated with widely different parts of the system. But if the second damper instead is placed close to the first one, they are likely to interact in the damping of the same modes. The characteristics of this interaction is less obvious. In this chapter, both types of locations will be studied.

In Section 8.1 a second damper is introduced in the spring-mass inter-area mode equivalent. Some generic cases for both local bus frequency and closest machine frequency feedback are given and are studied numerically. A useful finding is that tuning a damper using local bus frequency for maximum damping of a mode, is equivalent to impedance matching. This is shown through a comparison with an electric circuit, and can be used to explain the behaviour observed for the power systems in Section 8.3. But first Section 8.2 discusses possible dependencies between modes and dampers in larger systems. They motivate the use of routines that optimize an objective function but this hides the dependencies between specific modes and gains. As understanding is more important than optimality here, other methods are chosen: for the three machine system the modes are studied separately when varying the two gains. For the twenty-three machine system all eigenvalues are followed but only one gain is varied at a time. Section 8.3 thus explores the impact of two dampers on the three machine system. This gives valuable information on damper interaction in a meshed network, which makes it possible to interpret the results for the twenty-three machine system in Section 8.4. After studying two dampers that both aim at Modes 1 and 2, one of them is replaced by a damper that instead improves the damping of Mode 3. The conclusions of the chapter are given in Section 8.5.

8.1 Spring-Mass Inter-Area Mode System

The use of two dampers requires two control inputs at separate locations in the network. In the spring-mass model of Fig. 8.1 this corresponds to the force inputs F_3 and F_4.

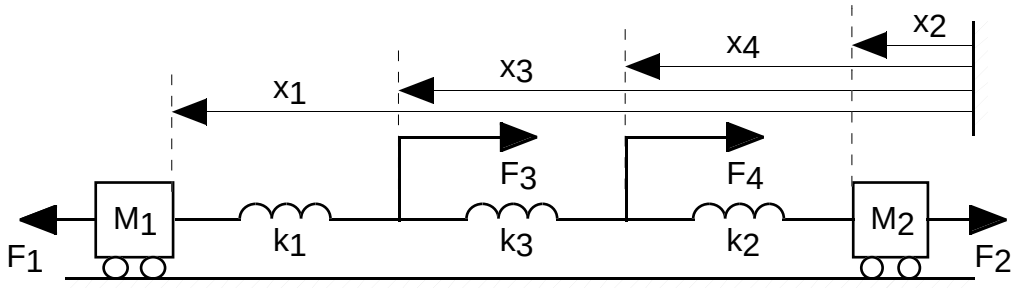

Fig. 8.1 Spring-mass inter-area mode system with force inputs.

In the following it is convenient to view the three springs as parts of one spring with spring coefficient k. First assume that F_3 and F_4 are zero. By letting the spatial coordinates a and b specify the points x_3 and x_4 *relative* to the distance from x_1 to x_2 respectively, the joint spring is divided into three parts being a, b-a and 1-b of the full length:

$$\frac{1}{k_1}=\frac{a}{k};\quad \frac{1}{k_3}=\frac{b-a}{k};\quad \frac{1}{k_2}=\frac{1-b}{k};$$

It is easy to show that the three springs coupled together yield a spring with the spring coefficient k,

$$\frac{1}{k_1}+\frac{1}{k_2}+\frac{1}{k_3}=\frac{1}{k}$$

Changing a and b to relocate the forces F_3 and F_4 will not alter the resonance frequency,

$$\sqrt{k\left(\frac{1}{M_1}+\frac{1}{M_2}\right)} \tag{8.1}$$

which can be compared to (2.30). Whereas eigenvalues and zeroes of the uncontrolled system could be determined analytically, the behaviour for finite gains require numeric treatment. This is done below for feedback from local bus frequency and from the frequency of the closest machine.

The candidate location with the highest mode controllability is chosen for the first damper. The mode controllability of the second damper is consequently lower.

Local Bus Frequency

As shown in Section 4.3 feedback from local bus frequency to active power is equivalent to a viscous damper in the spring-mass model. Two dampers thus give the system in Fig. 8.2.

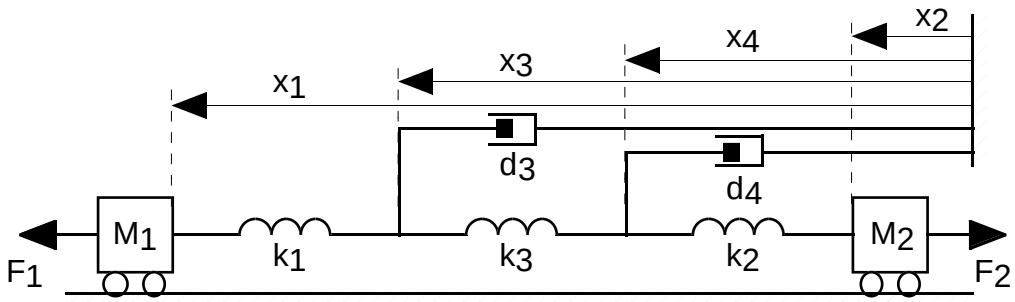

Fig. 8.2 Spring-mass inter-area mode system with two dampers.

F_1 and F_2 are omitted as they are constant and will not affect the dynamics. To demonstrate the relationship between damping and the parameters, some numerical values are chosen: M_1, M_2 and k are 1 kg, 4 kg and 5 N/m respectively, giving a resonance frequency of 2.5 rad/s. The location a of the first damper is set to 0.4. This gives a root locus for a varying d_3 and zero d_4 similar to the right graph of Fig. 7.2. This behaviour is also representative of Figs 7.6, 7.8 and 7.9.

The mode controllability of the first and second dampers at the locations a and b are obtained by entering the appropriate spring coefficients into (3.5),

$$\frac{\kappa}{\lambda_1}\frac{\frac{k}{aM_1}-\frac{k}{(1-a)M_2}}{\frac{k}{a}+\frac{k}{(1-a)}};\quad \frac{\kappa}{\lambda_1}\frac{\frac{k}{bM_1}-\frac{k}{(1-b)M_2}}{\frac{k}{b}+\frac{k}{(1-b)}};$$

The value a=0.4 gives a mode controllability of 0.5 κ/λ_1. Two locations of the second damper are used; b=0.5 and b=0.99. The mode controllability is then 0.375 κ/λ_1 and -0.2375 κ/λ_1 respectively.

The root locus method is not applicable as the dependence on two parameters is to be studied. Instead the real part of inter-area mode eigenvalues is plotted as a function of the two gains as in Fig. 8.3.

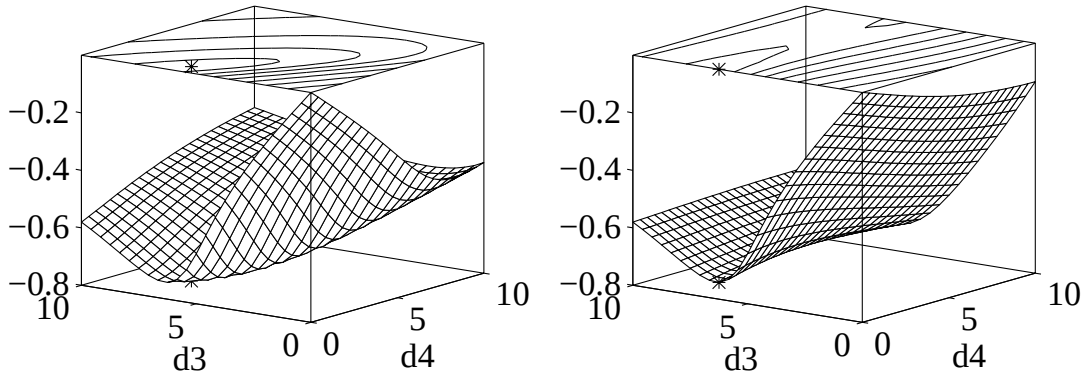

Fig. 8.3 Real part of the inter-area mode eigenvalues as the gains are varied between 0 and 10. The parameter *a* is 0.4, while *b* takes the values 0.5 (left) and 0.99 (right). '*' indicates the point of maximum damping.

At low gains, both dampers contribute to damping and as expected the first damper is more effective than the second. The maximum damping with both dampers in operation is only slightly better than that of the first damper alone.

This behaviour can be understood by introducing an electric equivalent based on the analogies in Table 8.1 from [Peterson 1996].

Electrical System	Mechanical System
Voltage *u*	Velocity *v*
Current *i*	Force *F*
Capacitor *C*	Mass *M*
Inductance *L*=1/*k*	Spring coefficient *k*
Conductance *G*	Viscous damping *d*

Table 8.1 Equivalent variables and parameters in mechanical and electrical systems.

Application of the analogies to the equations governing the system in Fig. 8.2 gives a state space description that agrees with the circuit of Fig. 8 .4.

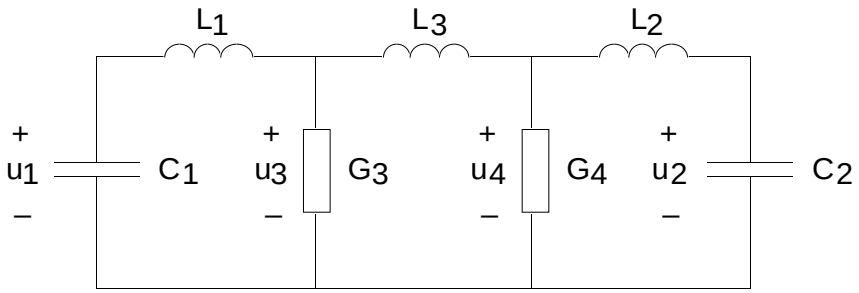

Fig. 8.4 Electric equivalent to the spring-mass inter-area mode system with two dampers.

The conductances G_3 and G_4 represent the dampers. If these parameters are zero, the electric system is a pure LC-circuit. It exhibits an undamped oscillatory mode with the frequency,

$$\frac{1}{\sqrt{L_{tot}C_{tot}}} = \sqrt{\frac{1}{L_1 + L_2 + L_3}\left(\frac{1}{C_1} + \frac{1}{C_2}\right)}$$

which is equivalent to the expression (8.1). Setting G_3 to infinity yields two LC-circuits with different resonance frequencies. This corresponds to the mechanical system zeroes in Fig. 7.1. The dynamic behaviour of the electric circuit thus agrees with that of the mechanical system.

For this circuit active and reactive power are well-defined: active power is dissipated in the conductances, while reactive power quantifies the energy oscillating between the lossless inductors and capacitors. Consequently the oscillation is damped as its energy is *dissipated* as active power. This view of oscillations and damping is also discussed for vibration damping [Ekdahl 1996].

If only the damper G_3 is considered, maximum damping is equal to maximizing the active power P_3 dissipated in the damper. This agrees with previous experience as zero and infinite G_3 both yield zero damping since in the first case the current is zero, while in the second case the voltage is zero. By modelling the circuit as G_3 connected to a two-pole with impedance Z, the condition for maximum P_3 is conveniently formulated as that of *impedance matching*,

$$\frac{1}{G_3} = |Z| \tag{8.2}$$

If G_3 is matched to the rest of the circuit and L_3 is zero, it is obvious that introducing G_4 will decrease damping. If L_3 is greater than zero G_4 will disturb G_3 less and some active power can be dissipated in G_4. This agrees well with the results for the spring-mass system in Fig. 8.3. In this case the mode controllability of the second damper is lower. The limited improvement due to the second damper is therefore expected. It is obvious that the concept of impedance matching is relevant for qualitative analysis.

Direct use of (8.2) is more complicated as the impedances of capacitances and inductances involve a frequency. An iterative procedure is required as the frequency is obtained from the eigenvalues which are affected by the conductance, that was to be determined. The pseudo code below suggests one solution:

$G=G_0$
`while` $|\Delta G|>\varepsilon$
    ω = mode frequency for the current value of G
    $\Delta G=G\text{-}1/|Z(\omega)|$
    $G=G+\alpha\Delta G$
`end`

The routine was applied to the selection of G_3 in Fig. 8.4 with G_4=0. The system parameters were chosen so that this is equivalent to the selection of d_3 in Fig. 8.2 with d_4=0. Using the imaginary part of the inter-area mode eigenvalue as ω and letting $10^{-3}<G_0<40$, α=0.1, $\varepsilon=10^{-4}$, the procedure converges to G_3=6.75 with the eigenvalues -0.738±j2.985. If instead ω is taken as the absolute value of the inter-area mode eigenvalue the gain G_3=6.09 gives the eigenvalues -0.738±j2.861. Looking closer at Fig. 8.3 for d_4=0, the gain 6.4 yields the best damping by placing the eigenvalues at -0.743±j2.922. Despite the numerical discrepancy, the concept of impedance matching is valuable as it provides a condition for maximum damping that has a physical interpretation.

Measured Closest Machine Frequency

The equivalent to machine frequency in Fig. 8.1 is velocity of the masses. In order to determine which mass is the closest to the damper location, the point of zero mode controllability needs to be known. Using the same values of M_1, M_2 and k as above it occurs if either a or b is set to 0.8. The first damper is located at a=0.4 and F_3 is thus controlled in proportion to v_1 with the gain d_3. For the values 0.5 and 0.99 of b, the proper feedback signals are v_1 and v_2 respectively. The gain of the second damper is d_4 and its output is F_4. Varying the two gains independently and plotting the real part of the inter-area mode eigenvalues gives Fig. 8.5.

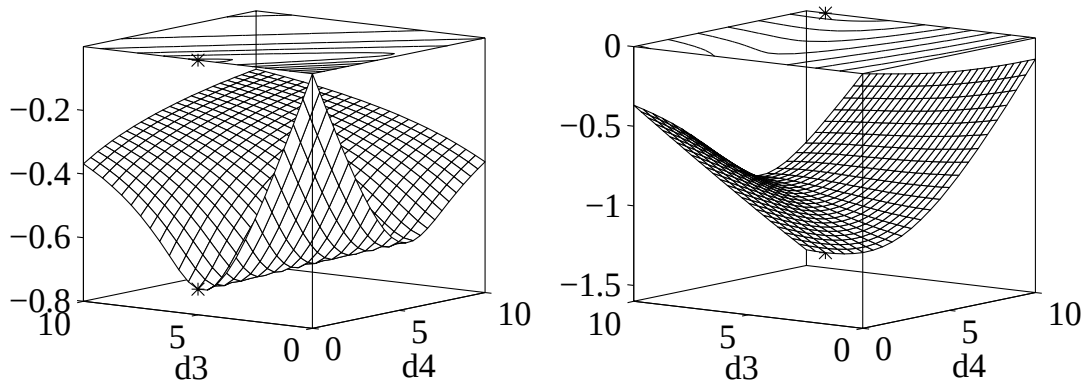

Fig. 8.5 Real part of the inter-area mode eigenvalues as the gains are varied between 0 and 10. The parameter a is 0.4, while b takes the values 0.5 (left) and 0.99 (right). '*' indicates the point of maximum damping.

The results for the two values of b differ substantially. When both dampers are associated with the same machine and the first damper is tuned for maximum damping, the second damper can not add any damping. If the dampers instead are associated with different machines their joint operation yields very high damping.

The structural properties of the zeroes described in Section 7.1 may explain the effect of the second damper. An infinite d_3 brings the inter-area mode eigenvalues to the zeroes, that according to [Miu 1991] can be obtained by fixing the actuator and the sensor. This gives constant values of both x_1 and x_3 and moves the swing node to x_3. A finite d_3 will not fix x_1 and x_3, but reduce the magnitude of their excursions. In both cases the first damper alone can damp the motions of M_1. Whereas the most active mass is M_1 in the uncontrolled system, it is M_2 once M_1 is damped.

Placing the second damper at b=0.5 with feedback from v_1 leads to a situation much like for the local bus frequency case, where the second damper disturbs the first damper rather than supports it.

If instead the second damper is located at b=0.99 with feedback from v_2, it acts to damp M_2. With one damper at each mass Fig. 8.5 indicates that there is no limit for the real part of the inter-area mode eigenvalues.

8.2 Interaction and Selection of Gains

By considering the geographical extent of the electro-mechanical modes, they can be categorized as more or less local. The fact that local modes in different parts of the system are unlikely to interact offers a certain amount of decoupling. Similarly, most damper locations will affect only a few modes. This was shown in Chapter 7, where only Modes 1 and 2 were influenced by the suggested dampers. Selection of gains in many dampers that affect many modes can therefore often be divided into a number of *independent* subproblems that involve fewer dampers and modes. When all the possibilities of decoupling have been exhausted, the problems cannot be further simplified and their complexity can then be categorized according to Table 8.1.

	One mode	Many modes
One damper	Case 1	Case 2
Many dampers	Case 3	Case 4

Table 8.2 Dependencies between modes and dampers leading to four cases.

If each damper influences only one mode and each mode is affected by only one damper (Case 1), the selection of each gain can be treated separately. The root locus method is well suited for the selection of one parameter as shown in Chapter 7. There it was evident that several modes could be affected by one gain (Case 2), and that they reached maximum damping at different values of this gain.

The influence on many modes calls for a measure of their joint performance, known as an *objective function*. Having defined an appropriate objective function, the gain selection problem may be submitted to an optimization routine. One example of an objective function is the real part of the least damped eigenvalue. Another example is to use the sum (of the real parts) of the eigenvalues computed as the *trace* of the system matrix [Eliasson and Hill 1992]. The success of an optimization routine depends critically on the choice of the objective function.

Coordinated selection of several gains (Cases 3 and 4) is considerably more complicated than selecting a single gain. This is particularly true for Case 4. As mentioned above an optimization routine can search the parameter space for a set of gains that optimizes the objective function. An alternative is the method based on discretization of a part of the parameter space that was used above. This may be applied to each mode of a larger system, provided the modes are sufficiently few and can be kept apart. Since this is the case for the three machine system the influence of two dampers will be studied using this method. If the number of modes is large or if they cannot be separated they are replaced by an objective function, which however hides the individual modes. For larger systems such as the twenty-three machine system, neither of these methods therefore contributes much to the understanding of the dependencies between modes and gains.

A preferred alternative is to select the gains one at a time using root locus plots. This gives a good insight in system behaviour, which is given priority here. A drawback of sequential optimization or uncoordinated gain selection is that the final set of selected gains is very unlikely to be optimal. Fig. 8.3 on the other hand shows two minima on each side of a saddle point. This indicates that also coordinated gain selection by unconstrained optimization may have problems minimizing the real part of the mode.

8.3 Three Machine System

In Chapter 7 bus N8 was chosen as the location of the first damper as it offered superior mode controllability of the 1.3 Hz mode according to Table 3.1. The mode controllability of the 1.8 Hz mode at bus N8 was

exceeded only by bus N6, which therefore is the natural location for the second damper.

Local Bus Frequency

The eigenvalue sensitivities at zero gain in Table 7.1 indicate that active power controlled by the local bus frequencies both at N6 and N8 initially increase the damping of the two modes. Damping for nonzero gains is shown in Fig. 8.6. It shows for each mode the real part of the electro-mechanical eigenvalue as a function of the two damper gains d_6 and d_8. Note that the dependence on the gain d_8 for d_6=0 is illustrated more in detail in Fig. 7.6.

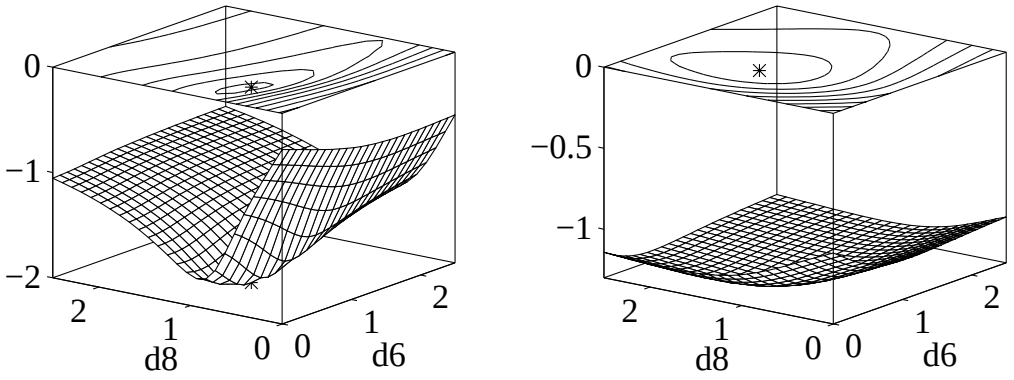

Fig. 8.6 Real parts of the 1.3 Hz mode (left) and the 1.8 Hz mode (right) for different gains of the dampers at bus N6 and N8 using feedback from local bus frequency.

The damping of both modes increases with the gains as long as they are small, but for sufficiently large gains damping decreases again. The joint operation of the dampers has different influence on the two modes. Starting out from optimum damping of the 1.3 Hz mode due to the damper at N8, the damper at N6 cannot offer much improvement. This behaviour is close to that of the spring-mass system with b=0.5 analyzed above.

Damping of the 1.8 Hz mode more symmetrically depends on the gains of both dampers. This is different from the spring-mass case, but the inter-area mode model is one-dimensional. The meshed nature of the three machine system is thus qualitatively different and cannot be explained by the simple spring-mass model. By assigning a direction to the modes the damper locations can be related to this direction. Upwards in Fig. 2.5 is now defined as North. Using Fig. 4.3 the direction of the 1.3 Hz mode is North-South, while that of the 1.8 Hz mode is Northeast-Southwest. It can now be concluded that the influence of two dampers *along* the swing direction can be described by the spring-mass model. Two dampers that are

not electrically close to each other and are located *side by side* in the swing direction cannot be incorporated in the spring-mass model of Fig. 8.1. From Fig. 8.6 it is evident that these two dampers together yield more damping than any of them on its own.

Fig. 7.6 also shows eigenvalues of a third complex mode moving towards the imaginary axis. For high gains, the eigenvalues of this mode may have the smallest real part. When selecting the gains, it therefore seems reasonable to use the real part of the least damped mode as an objective function that should be minimized. The variation of this quantity as a function of the gains d_6 and d_8 is illustrated in Fig. 8.7.

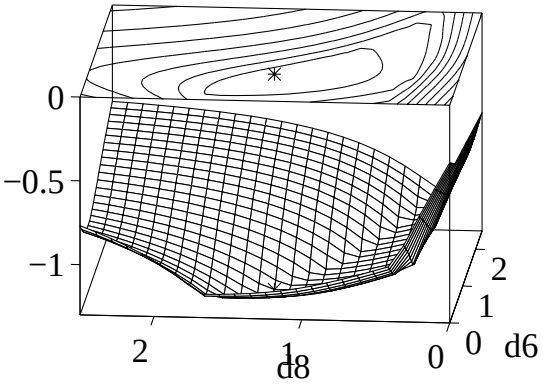

Fig. 8.7 Real part of the least damped oscillatory mode for different gains of the dampers at bus N6 and N8 using feedback from local bus frequency. The point of maximum damping is indicated by '*'.

For small values of the gains, the 1.3 Hz mode is the least damped. Somewhat larger gains make the 1.8 Hz mode the least damped, while for large gains it is the third mode. The objective function has its minimum at d_6=0.73 and d_8=1.25 p.u./(rad/s) which gives the complex eigenvalues -1.3±j11.7, -1.4±j9.6 and -1.3±j5.8.

Measured Closest Machine Frequency

According to the methods in Section 4.4 for finding the closest machine, S3 is closest to bus N6. Fig. 3.3 leaves little doubt about this, but to be certain Table 8.3 may also be consulted. It contains the eigenvalue sensitivity of the electro-mechanical eigenvalues to feedback from machine frequency to active power at N6. Table 8.3 verifies that feedback from the machine S3 is the only alternative with appropriate argument for both modes.

Machine	1.3 Hz mode	1.8 Hz mode
H1	$0.509e^{j5°}$	$0.098e^{j12°}$
S2	$1.504e^{-j172°}$	$0.966e^{-j4°}$
S3	$0.909e^{-j170°}$	$3.245e^{-j176°}$

Table 8.3 Eigenvalue sensitivity of the electro-mechanical eigenvalues in the second quadrant to feedback from machine frequency to active power at bus N6.

Fig. 8.8 illustrates how the damping of the modes depend on the gains d_6 and d_8 of the dampers located at bus N6 and N8.

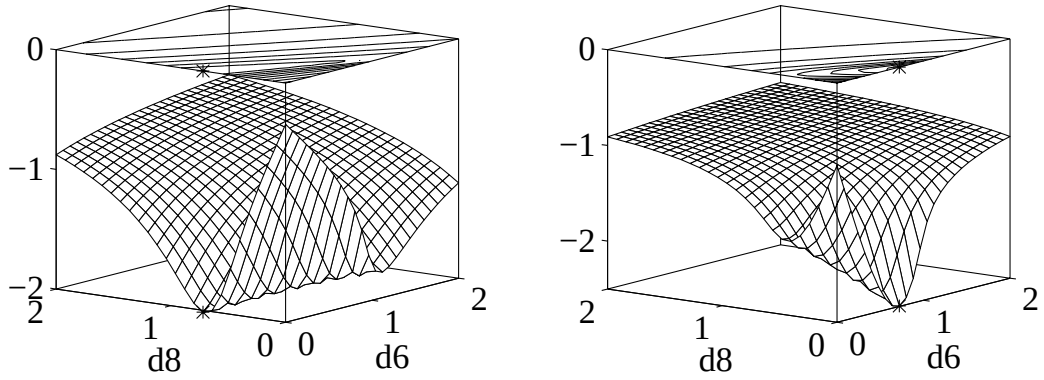

Fig. 8.8 Real parts of the 1.3 Hz mode (left) and the 1.8 Hz mode (right) for different gains of the dampers at bus N6 and N8 using feedback from the frequency of S3. The point of maximum damping is indicated by '*'.

Just like for the spring-mass model with b=0.5, one measurement signal here controls two actuators. It is therefore natural that the results are very similar to those in Fig. 8.5 for b=0.5: provided the damper at the location with the highest mode controllability is tuned for maximum damping, the other damper can only reduce damping. Letting one gain be zero, damping depends on the other gain much like in the bus frequency case. It indicates that although not directly applicable, impedance matching may be relevant for feedback from machine frequency. This is natural as good damping also in this case is a balance between the magnitude of the actuator output and the feedback signal that are increased by high and low gains respectively.

Machine frequency as feedback signal does not give rise to a third complex mode. Fig. 8.9 shows that for small and large gains the least damped mode is the 1.3 Hz mode, while for intermediate gains it is the 1.8 Hz mode. Selecting the gains by minimizing the real part the least damped mode yields the point indicated by '*' in Fig. 8.9. It occurs at d_6=0.88 pu/(rad/s) and d_8=0.08 pu/(rad/s) which gives the complex eigenvalues -1.8±j9.2 and -1.8±j7.6.

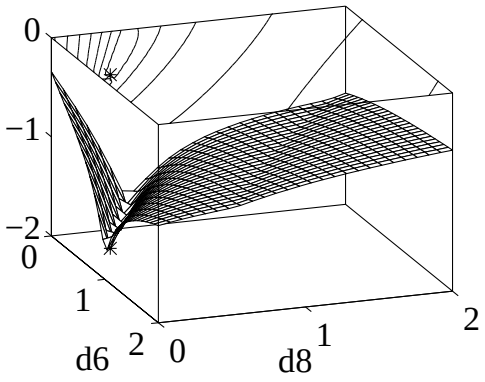

Fig. 8.9 Real part of the least damped oscillatory mode for different gains of the dampers at bus N6 and N8 using feedback from the frequency of S3. The point of maximum damping is indicated by '*'.

8.4 Twenty-three Machine System

The twenty-three machine system is sufficiently large to contain both inter-area modes such as Mode 1 and more or less local electro-mechanical modes. Most modes will involve only a part of the system and are consequently affected only by dampers within the corresponding area. This is the case for Modes 2 and 3. The fact that Modes 1 and 2 are affected by dampers both at bus N51 and at bus N63, raises the question of controller interaction. This is studied here by departing from the cases in Section 7.4 with one damper and adding a damper at the other location. The influence of the new damper can then be studied in a root locus plot. Together with Section 7.4, this gives information about system behaviour along four lines in the two-dimensional parameter space spanned by the two gains as illustrated in Fig. 8.10. Results for the lines on the axes are presented in Section 7.4, while the other two are explored below.

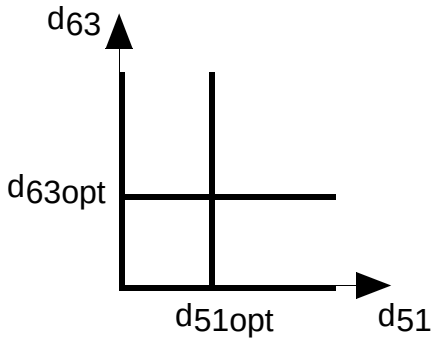

Fig. 8.10 Explored parts of the parameter space spanned by the gains d_{51} and d_{63} of the dampers at bus N51 and bus N63. $d_{51\text{opt}}$ and $d_{63\text{opt}}$ are the optimum gains selected in Section 7.4.

As the first damper modifies system dynamics, sensitivities based on the measures of mode observability and mode controllability in Chapters 3 and 4 are no longer valid. Therefore new sensitivities are computed for the cases with one damper at optimum gain.

A single damper at bus N51 or bus N63 gives sufficient damping to Modes 1 and 2, but Mode 3 is hardly affected by dampers at these locations. A second damper is therefore introduced at a new location in order to increase the damping of Mode 3.

Local Bus Frequency

The root locus plots of Figs 7.8 and 7.9 indicated that suitable gains for active power controlled by local bus frequency at bus N51 and N63, are 2.8 and 4 p.u./(rad/s) respectively. These gains bring Mode 1 to its point of maximum damping, while Mode 2 could be even better damped by higher gains.

Assuming that the damper at bus N51 has its gain d_{51} set to 2.8 p.u./(rad/s), the eigenvalue sensitivity to feedback gains at this point is of interest. In Table 8.4 values are given for the buses N51 and N63, but also for N1042 and N47 where the sensitivity of Mode 3 is highest.

Bus	Mode 1	Mode 2	Mode 3
N1042	$0.114e^{j161°}$	$0.078e^{-j69°}$	$0.140e^{-j172°}$
N47	$0.036e^{-j157°}$	$0.009e^{j62°}$	$0.115e^{-j172°}$
N51	$0.251e^{j77°}$	$0.537e^{j176°}$	$0.002e^{j158°}$
N63	$0.321e^{-j160°}$	$0.080e^{j52°}$	$0.055e^{j178°}$

Table 8.4 Sensitivities of the selected eigenvalues in the second quadrant to local feedback from bus frequency to active power when d_{51} is 2.8 p.u./(rad/s).

According to Fig. 7.8, an increase in d_{51} moves the eigenvalue in the second quadrant of Mode 1 upwards, while those of Modes 2 and 3 are further damped. This agrees well with Table 8.4, which also states that the damper at N63 initially will improve the damping to Modes 1 and 3, while actually decreasing that of Mode 2. This is verified by Fig. 8.11 which shows the root locus for a variation in d_{63} when d_{51} is 2.8 p.u./(rad/s).

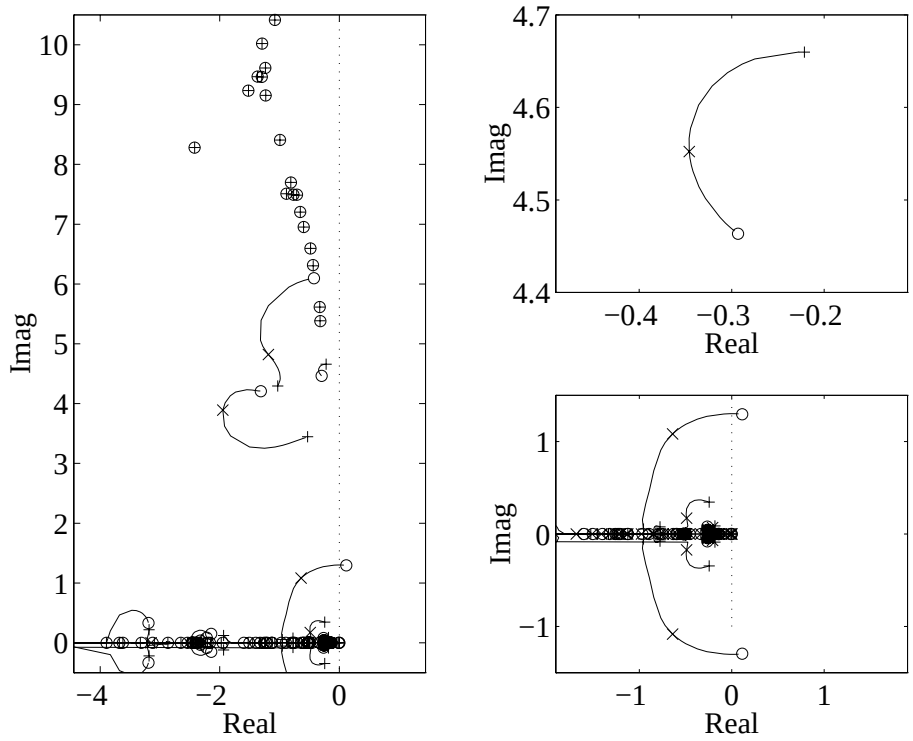

Fig. 8.11 Root locus for the gain d_{63} that relates active power injection at bus N63 with local bus frequency. Eigenvalue locations for the values zero (+), 4.6 (x) and infinity (o) of d_{63} are indicated while d_{51} constantly is 2.8 p.u./(rad/s). The right graphs shows details of the left plot.

Before interpreting Fig. 8.11, the fourth line of Fig. 8.10 is explored by setting d_{63} to its optimum value of 4 p.u./(rad/s) while d_{51} temporarily is zero. This gives the eigenvalue sensitivities to feedback from local bus frequency to active power injection. Table 8.5 contains the values both for the buses N51, N63 and N1042 as well as for N47 where the sensitivity of Mode 3 is high.

Bus	Mode 1	Mode 2	Mode 3
N1042	$0.218e^{-j132°}$	$0.139e^{j109°}$	$0.058e^{-j142°}$
N47	$0.072e^{-j129°}$	$0.058e^{j79°}$	$0.119e^{-j163°}$
N51	$0.407e^{-j144°}$	$0.159e^{j108°}$	$0.076e^{j150°}$
N63	$0.413e^{j92°}$	$0.346e^{-j172°}$	$0.004e^{-j2°}$

Table 8.5 Sensitivities of the selected eigenvalues in the second quadrant to local feedback from bus frequency to active power when d_{63} is 4 p.u./(rad/s).

The sensitivities to a feedback gain at bus N63 agree well with the root locus of Fig. 7.9. The same comparison but for bus N51 can be done with

Fig. 8.12. It is the root locus obtained by varying d_{51} when d_{63} is 4 p.u./(rad/s).

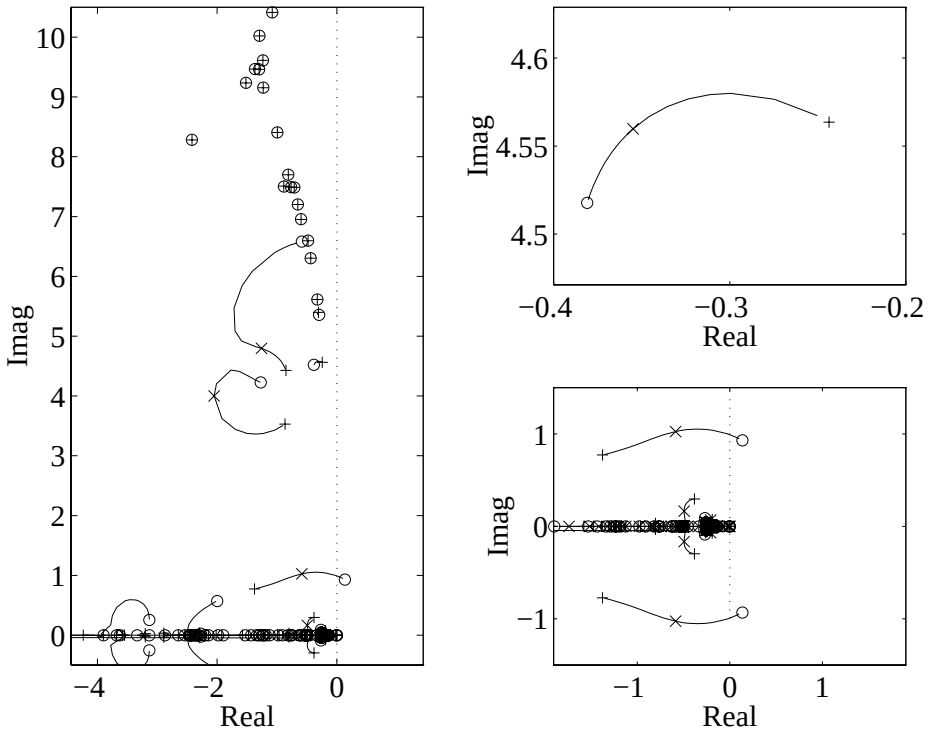

Fig. 8.12 Root locus for the gain d_{51} that relates active power injection at bus N51 with local bus frequency. Eigenvalue locations for the values zero (+), 3.6 (x) and infinity (o) of d_{51} are indicated while d_{63} constantly is 4 p.u./(rad/s). The right graphs shows details of the left plot.

By combining the mode shapes in Fig. 2.9a with the swing patterns in Fig. 2.9b the geographical extent and direction of the modes can be characterized. Mode 1 is a global North-South mode, while Mode 2 is a more local mode where the machines at A4051 swing against those at A4047 and A4063.

Relative to the swing direction of Mode 1, N51 and N63 are located side by side just like the buses N6 and N8 for the 1.8 Hz mode of the three machine system. By looking at Fig. 8.6 it is therefore expected that the dampers at N51 and N63 together yield more damping than any of them can provide on its own.

The locations of N51 and N63 relative to the swing direction of Mode 2 are comparable to those of N6 and N8 for the 1.3 Hz mode of the three machine system. Figs 8.6 and 7.8 show that in both cases (close to) maximum damping is obtained by using only the damper at the superior

location which here is N51. If the gain of this damper is less than required for maximum damping, the other damper can improve damping as shown both in Figs 8.6 and 8.11. The damper at N51 can also support the one at N63, especially if the gain of the latter is not selected for maximum damping of the mode.

The results in Section 7.4 for one damper alone are very good, and show that one damper at bus N51 or N63 can add sufficient damping to Modes 1 and 2. Of the two alternatives, the damper at N63 with gain d_{63} set to 4 p.u./(rad/s) is chosen as it provides more damping of Mode 1. The eigenvalue shifts that are achieved through joint operation of the two dampers are unrealistically large. Instead of further damping Modes 1 and 2, a second damper is dedicated for damping of Mode 3.

Table 8.5 reveals that Mode 3 exhibits the greatest sensitivity to feedback from local bus frequency to active power at bus N47. The root locus for variations in the gain d_{47} is shown in Fig. 8.13.

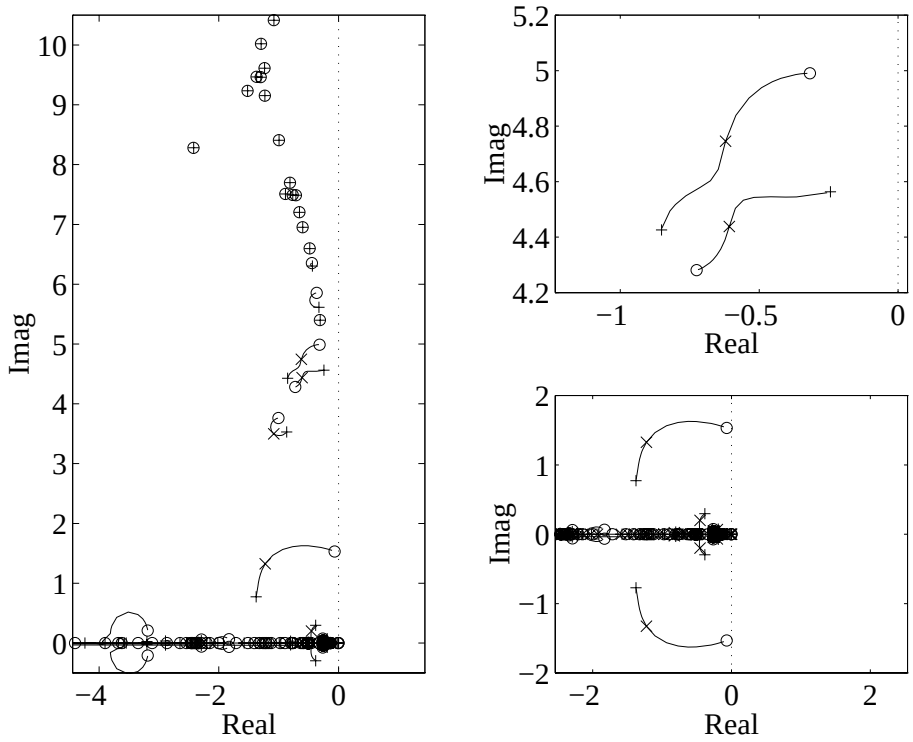

Fig. 8.13 Root locus for the gain d_{47} that relates active power injection at bus N47 with local bus frequency. Eigenvalue locations for the values zero (+), 2.8 (x) and infinity (o) of d_{47} are indicated while d_{63} constantly is 4 p.u./(rad/s). The right graphs shows details of the left plot.

It is evident that the damping of Modes 1 and 3 is improved by the new damper, whereas that of Mode 2 is decreased. The value 2.8 p.u./(rad/s) of d_{47} gives a reasonable compromise and is indicated in the plot.

Fig. 8.13 shows that the branches of Modes 2 and 3 start out as semi-circles. Having come halfway after passing the suggested value of d_{47}, they however switch roles and follow each others' semi-circles towards the zeroes. This strong interaction is probably due to similar mode shapes and close eigenvalue locations as mentioned in connection with Fig. 7.12. The individual dependence of Modes 2 and 3 on the gain d_{47} will not be commented.

It is interesting to note that the poorly damped zeroes corresponding to a rigid body mode are stable in Fig. 8.13 in contrast to those in Figs 7.8, 7.9, 8.11 and 8.12. Locating the dampers at the buses N47 and N63 better reflects the extent of the rigid body mode and thereby seems to enable damping of it.

Measured Closest Machine Frequency

According to Figs 7.12 and 7.13 active power injection at the buses N51 or N63 controlled by the machine frequency of A4051_1 and A4063_1 respectively could provide good damping of Modes 1 and 2. Setting the gain d_{51} of the damper at N51 to 2.4 p.u./(rad/s) gave maximum damping of Mode 1, while Mode 2 could be further damped by a higher value. By instead using the damper at N63 with its gain d_{63} set to 2.6 p.u./(rad/s) the damping of Mode 2 was instead at its peak, while the damping of Mode 1 would benefit from a higher gain.

The same procedure as for feedback from local bus frequency will now be followed to investigate the joint action of dampers both at bus N51 and bus N63. With d_{51} at its optimum value, the eigenvalue sensitivity to active power controlled by the frequency of the closest machine is calculated. Table 8.6 contains values for the buses N51 and N63, but also for those where the sensitivity of Mode 3 is highest which is N1042 and N47. At all these buses it is simple to determine the closest machine, which are A4051, A4063, A1042 and A4047. At plants with two units, number one is chosen.

Bus	Machine	Mode 1	Mode 2	Mode 3
N1042	A1042	$0.297e^{-j179°}$	$0.245e^{-j6°}$	$0.227e^{-j173°}$
N47	A4047_1	$0.067e^{-j121°}$	$0.057e^{j90°}$	$0.182e^{-j175°}$
N51	A4051_1	$0.945e^{j99°}$	$1.179e^{-j108°}$	$0.002e^{j170°}$
N63	A4063_1	$0.773e^{-j128°}$	$0.584e^{j75°}$	$0.103e^{j177°}$

Table 8.6 Sensitivities of the selected eigenvalues in the second quadrant to active power controlled by the frequency of the closest machine when d_{51} is 2.4 p.u./(rad/s).

The eigenvalue shift directions in Table 8.6 due to an increase of d_{51} agree well with those in Fig. 7.12. The corresponding values for d_{63} are verified by the root locus in Fig. 8.14, which is obtained by keeping d_{51} at 2.4 p.u./(rad/s) and varying d_{63}.

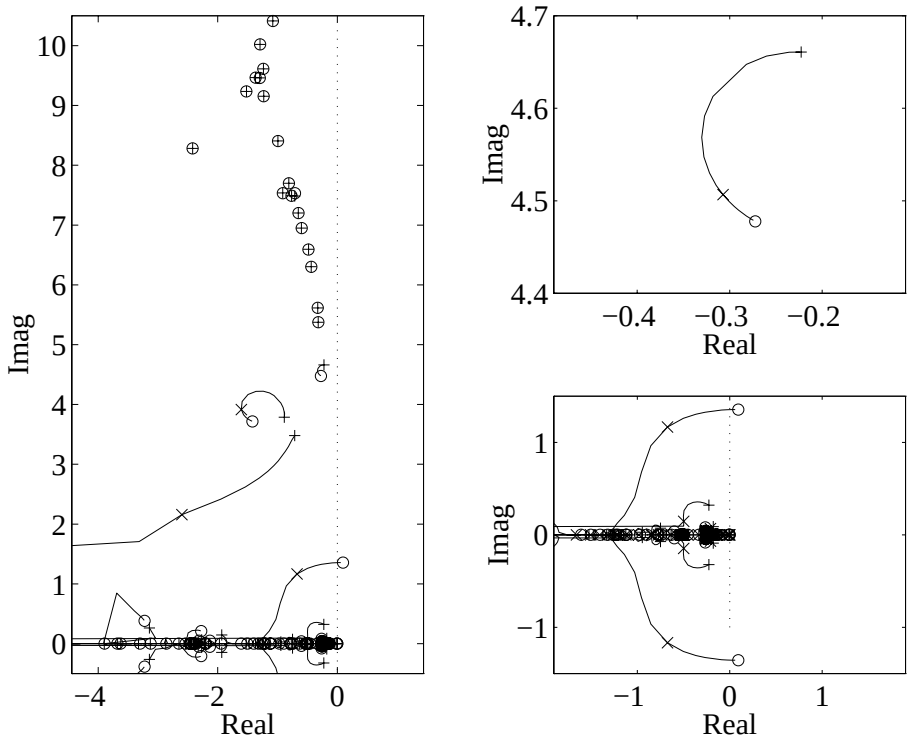

Fig. 8.14 Root locus for the gain d_{63} that relates active power injection at bus N63 with the frequency of the machine A4063_1. Eigenvalue locations for the values zero (+), 5.6 (x) and infinity (o) of d_{63} are indicated while d_{51} constantly is 2.4 p.u./(rad/s). The right graphs shows details of the left plot.

If instead d_{63} is set to its optimum value of 2.6 p.u./(rad/s) and d_{51} temporarily is set to zero, the new eigenvalue sensitivities to active power

controlled by the frequency of the closest machine result. The values for the four buses N1042, N47, N51 and N63 are given in Table 8.7.

Bus	Machine	Mode 1	Mode 2	Mode 3
N1042	A1042	$0.124e^{-j101°}$	$0.201e^{j145°}$	$0.110e^{-j153°}$
N47	A4047_1	$0.033e^{-j82°}$	$0.057e^{j110°}$	$0.199e^{-j169°}$
N51	A4051_1	$0.274e^{-j119°}$	$0.349e^{j154°}$	$0.095e^{j151°}$
N63	A4063_1	$0.385e^{j179°}$	$0.252e^{-j95°}$	$0.005e^{-j10°}$

Table 8.7 Sensitivities of the selected eigenvalues in the second quadrant to active power controlled by the frequency of the closest machine when d_{63} is 2.6 p.u./(rad/s).

Again the directions predicted for an increase of d_{63} agree with those seen in Fig. 7.13. Keeping d_{63} at its optimum value and varying d_{51} yields the root locus plot in Fig. 8.15.

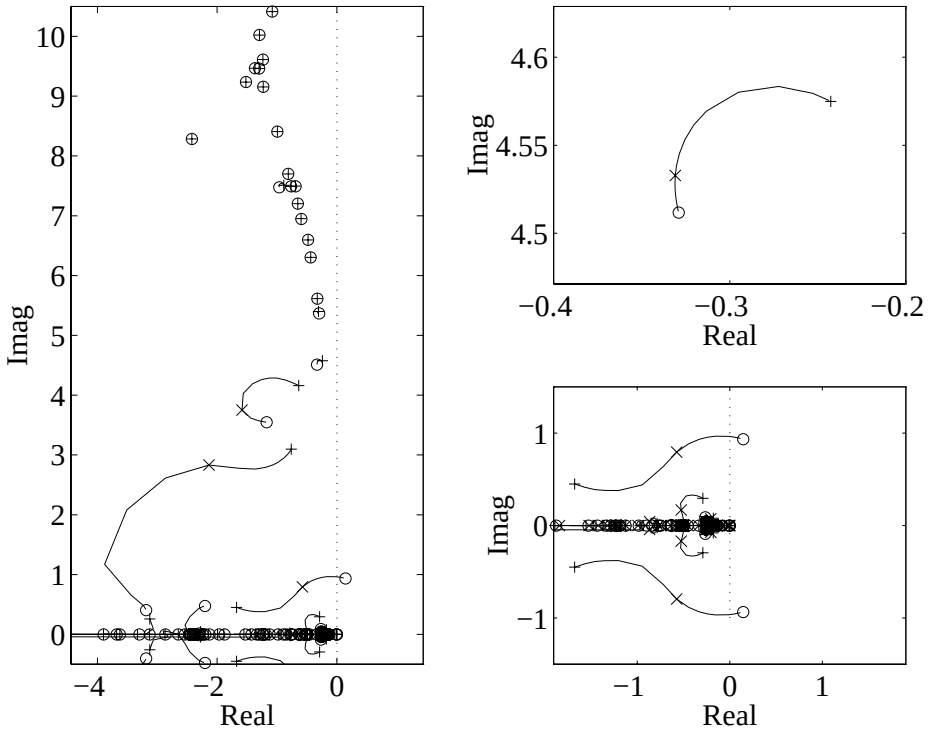

Fig. 8.15 Root locus for the gain d_{51} that relates active power injection at bus N51 with the frequency of the machine A4051_1. Eigenvalue locations are indicated for the values zero (+), 4.3 (x) and infinity (o) of d_{51} while d_{63} constantly is 2.6 p.u./(rad/s). The right graphs shows details of the left plot.

The plots in Figs 8.14 and 8.15 show that the use of two dampers can approximately double the damping of Mode 2, while it has even more effect on Mode 1. Whereas Fig. 7.13 also shows that Mode 1 can be fully damped, Fig. 7.12 suggests that this applies to Mode 2 instead. This proves the fact that in Fig. 7.12 these modes interact and have changed identities for values of d_{51} greater than 2.4 p.u./(rad/s).

Since the dampers at the buses N51 and N63 are associated with different machines, a comparison to the three machine system with two dampers is not valid. The behaviour of Mode 1 is much the same in Figs 8.14 and 8.15 as in Figs 7.12 and 7.13. Dampers at the two locations together thus influence Mode 1 in much the same way as they do on their own: the eigenvalues of Mode 1 can be pushed all the way down to the real axis, but at the same time other eigenvalues move towards a pair of unstable complex zeroes.

Mode 2 mainly includes the machines A4047, A4051 and A4063. Placing dampers close to two of these power plants is similar to using one damper in the spring-mass inter-area mode system. Each of the two dampers at N51 and N63 can therefore add damping to the mode, but as the machines at N4047 are free to move the total damping is limited.

Just like with feedback from local bus frequency, the use of a single damper gives sufficient damping of Modes 1 and 2. The damper located at bus N51 with feedback from the frequency at the machine A4051_1 is chosen as it gives the best damping of the two modes. According to Table 8.6, Mode 3 is most sensitive to active power injection at bus N1042 controlled by the frequency of the local machine A1042. The root locus for a variation of the gain d_{1042} is shown in Fig. 8.16

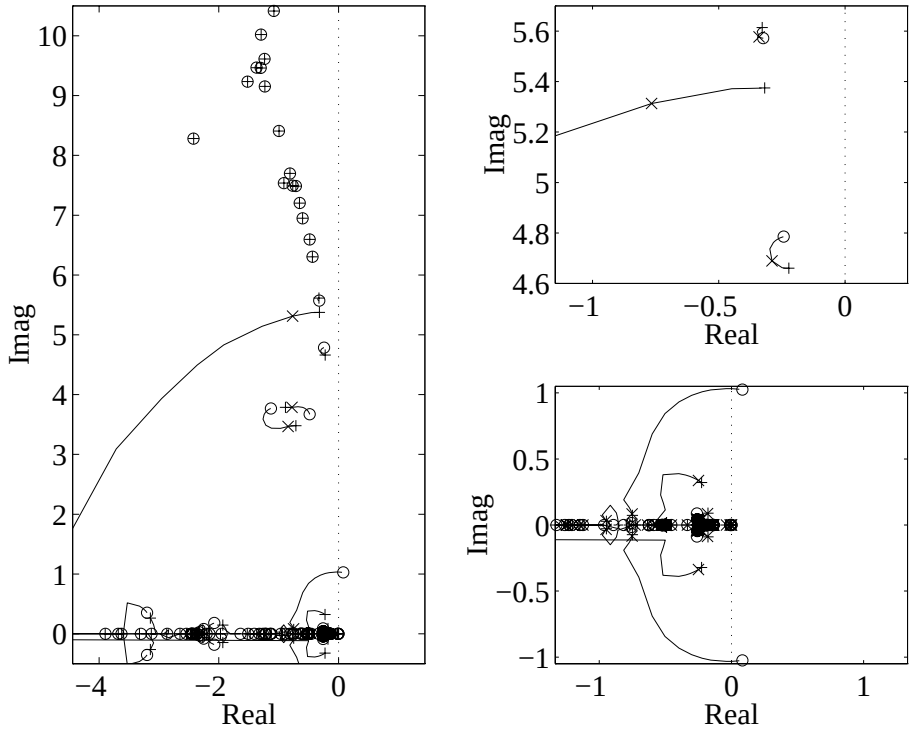

Fig. 8.16 Root locus for the gain d_{1042} that relates active power injection at bus N1042 with the frequency of the machine A1042. Eigenvalue locations are indicated for the values zero (+), 0.36 (x) and infinity (o) of d_{1042} while d_{51} constantly is 2.4 p.u./(rad/s). The right graphs shows details of the left plot.

Varying d_{1042} has great effect on a mode at 5.4 rad/s. Its mode shape shows machine A1042 swinging against the rest of the system, which explains the great impact. Despite the superior sensitivity to $d_{1042,}$ Mode 3 is hardly affected at all. The damper location A1042 is therefore rejected.

The second highest sensitivity of Mode 3 in Table 8.6 is to the gain d_{47}, that relates active power injection at bus N47 to the frequency of the machine A4047_1. Varying d_{47} when d_{51} is 2.4 p.u./(rad/s) gives the root locus in Fig. 8.17.

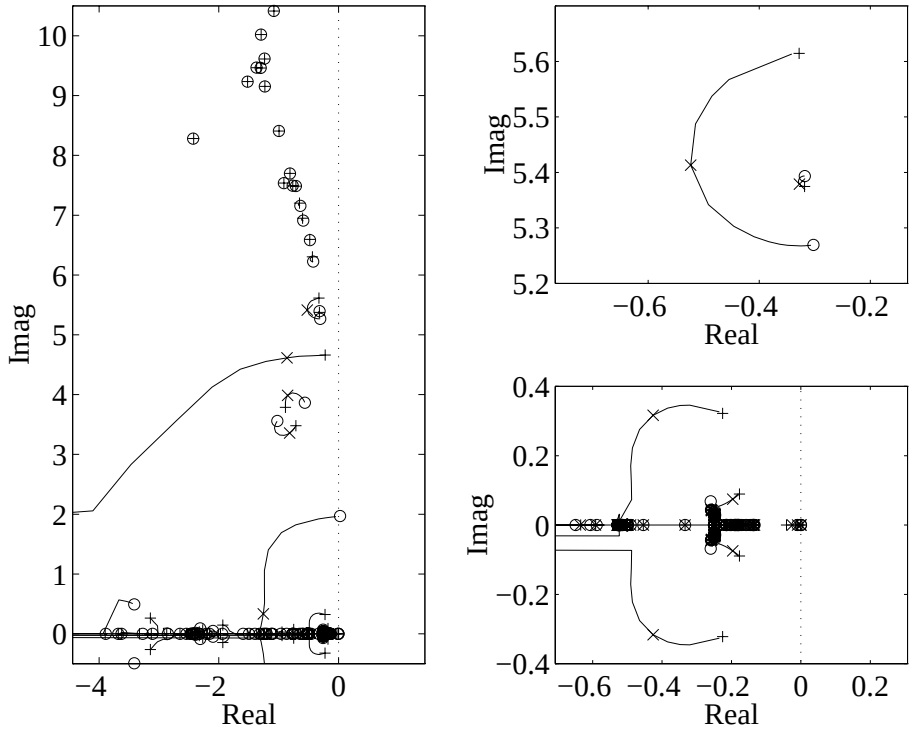

Fig. 8.17 Root locus for the gain d_{47} that relates active power injection at bus N47 with the frequency of the machine A4047_1. Eigenvalue locations are indicated for the values zero (+), 2.6 (x) and infinity (o) of d_{47} while d_{51} constantly is 2.4 p.u./(rad/s). The right graphs shows details of the left plot.

This time the damping of Mode 3 is increased considerably. As Modes 1 and 2 are less affected, it is fairly easy to select a suitable value of d_{47}, which is 2.6 p.u./(rad/s). This gives all three study modes the same real part -0.8, and actually improves damping of a faster 5.5 rad/s mode slightly.

8.5 Conclusions

The simple mechanical model again offers insight by providing understanding that is consistent with the behaviour of the more complex power systems. As predicted in the introduction to this chapter, a second damper can have either positive or negative effect on the damping of a certain mode.

For small gains, an increase in *any* gain will improve damping of the electro-mechanical modes.

For larger gains, the situation is more complicated but two cases may be distinguished. In the first case maximum damping of a mode is obtained by

using only one damper, while in the second it requires the joint operation of both dampers. The conditions can be summarized as below:

> If the feedback signal is local bus frequency and the dampers are located *along* the swing direction of the mode, the one with the highest mode controllability alone gives the best damping. The same applies for feedback from machine frequency if both dampers use the same feedback signal.
>
> When the dampers are placed *side by side* relative to the mode direction and local bus frequency is used for feedback, maximum damping is obtained by using both dampers. Similarly the use of two dampers can be more efficient than one, if the frequencies of different machines are used for feedback.

The negative influence on damping by a second damper can be explained by the fact that tuning of the first damper is equivalent to impedance matching provided the local feedback signal is employed. This is a consequence of characterizing the oscillations as reactive power and the damping effect as active power. Both these concepts are useful when analyzing power system damping, and especially when using active power as control signal.

The final damper locations in the twenty-three machine system for the bus frequency and machine frequency feedback cases are close. The resulting eigenvalue locations are also similar. This is natural since the points of measurement in the two cases differ very little, as compared to the distances involved.

The complex rigid body zeroes that were unstable in the single damper case, are stable (Fig. 8.13) or only slightly unstable (Fig. 8.17) when locating a damper at bus N47. Having dampers both here and at bus N51 or N63 gives damping to a larger part of the machines and thus improves damping even if one gain is infinite.

The eigenvalue sensitivity suggests that active power controlled by the closest machine frequency yields greater leverage on Mode 3 at bus N1042 than at bus N47. By tracing out the root locus bus N47 is proved to be superior. Together with the cases where modes with closely located eigenvalues interact and change identities, this demonstrates the complex nature of root locus branches. Studying the root locus plots, gives insight into what is required from an optimization routine that is to perform coordinated tuning of many dampers. Such knowledge may be useful when formulating a suitable objective function.